THE JOURNAL OF PHYSICAL CHEMISTRY B

Article

pubs.acs.org/JPCB

Auramine-O as a Fluorescence Marker for the Detection of Amyloid Fibrils

Nadav Amdursky[†,*] and Dan Huppert[‡]

[†]Department of Materials and Interfaces, Faculty of Chemistry, Weizmann Institute of Science, Rehovot, 76100, Israel

[‡]Raymond and Beverly Sackler Faculty of Exact Sciences, School of Chemistry, Tel Aviv University, Tel Aviv 69978, Israel

Supporting Information

ABSTRACT: There is an indispensable need for a fluorescence marker for the detection of amyloid fibrils, where, at present, the most used marker is thioflavin-T (ThT). Here, we present the use of auramine-O (AuO) as a possible alternative to ThT. As with ThT, the increase in the emission of AuO upon binding to amyloid fibrils is the result of inhibition of the free rotation of the two dimethylamino arms of the molecule. This inhibition prevents the excited-state electronic wave function from moving from the emissive locally excited state to the dark charge-transfer state. We further show that not only AuO is comparable to ThT as a fluorescent marker for amyloid fibrils but also it has a unique spectroscopic signature. AuO has distinct two modes that are characterized by a large shift in the absorption and emission peak positions between its unbound and bound states (before and after the fibrils formation, respectively). In this context, we show that, whereas the emission band position is red-shifting, the absorption peak shifts to the blue and the spectrum exhibits an isosbestic point. The large shifts in emission and absorption peak positions can be explained by the photoacid activity of AuO exhibiting an excited-state proton-transfer process.

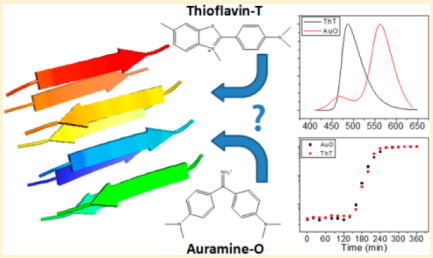

INTRODUCTION

Fluorescent sensors for amyloid fibrils have become an essential tool in biochemistry and biomedical research, mainly for the quantification of the potency of inhibitors for amyloid-related diseases, such as Alzheimer's disease, Parkinson's disease, amyloidosis, and others.[1−6] The fluorescent probe most used for amyloid fibrils is thioflavin-T (ThT). ThT binds to amyloid fibrils (a detailed review on the binding mechanism of ThT to amyloid fibrils can be found in[7]) thus increasing its fluorescence intensity by more than 2 orders of magnitude. Other molecules have been proposed to serve as fluorescent probes for amyloid fibrils, such as 4-(dicyanovinyl)-julolidine and 1-amino-8-naphtalene sulfonate; however, all of the proposed molecules have poorer spectroscopic sensitivity in comparison to ThT[8−10] or can markedly affect the amyloidogenesis process.[11]

The unique photophysical properties of ThT are a result of the rotation around a single C−C bond that connects the benzothiazole moiety to the dimethylanilino ring (Scheme 1). With the help of ab initio quantum-mechanical calculations it was shown that this rotation influences the electronically excited-state surface potential. The rotation about this bond causes the electronic wave function of the excited state to change from an emissive locally excited state to a nonradiative charge-transfer (CT) state.[12−15] The ab initio calculations were verified experimentally by changing the viscosity of the environment, which in turn affects the rotation of the internal bond.[14−21] The most suited nonradiative model that may explain the nonradiative processes of ThT seems to be one that was first introduced by Glasbeek and co-workers to explain the nonradiative processes of auramine-O.[22,23] It was later shown how this model can be successfully fitted to the photophysical properties of ThT as well.[12] This successful fitting begs the question whether AuO can also bind to amyloid fibrils, and consequently increasing its fluorescence intensity by several orders of magnitude. Historically, both ThT and AuO were first introduced as fluorescent markers more than 40 years ago.[24,25] Earlier than 2000, the photophysical properties of AuO have attracted more attention than those of ThT (Figure S1 of the Supporting Information). The main breakthrough in the use of ThT for the detection of amyloid fibrils was a consequence of the detailed protocol by LeVine for the quantification of amyloid fibrils by ThT.[4] Since then, the characterization of ThT gained much more attention than AuO (Figure S1 of the Supporting Information). In this communication, we show not only that AuO indeed increases its emission intensity upon binding to amyloid fibrils but also that its spectroscopic sensitivity is even superior to that of ThT.

Scheme 1. Molecular Schemes of Auramine O (Left) and Thioflavin T (Right)

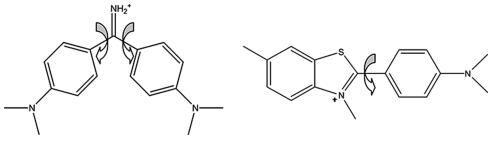

Received: October 16, 2012
Revised: October 22, 2012
Published: October 22, 2012

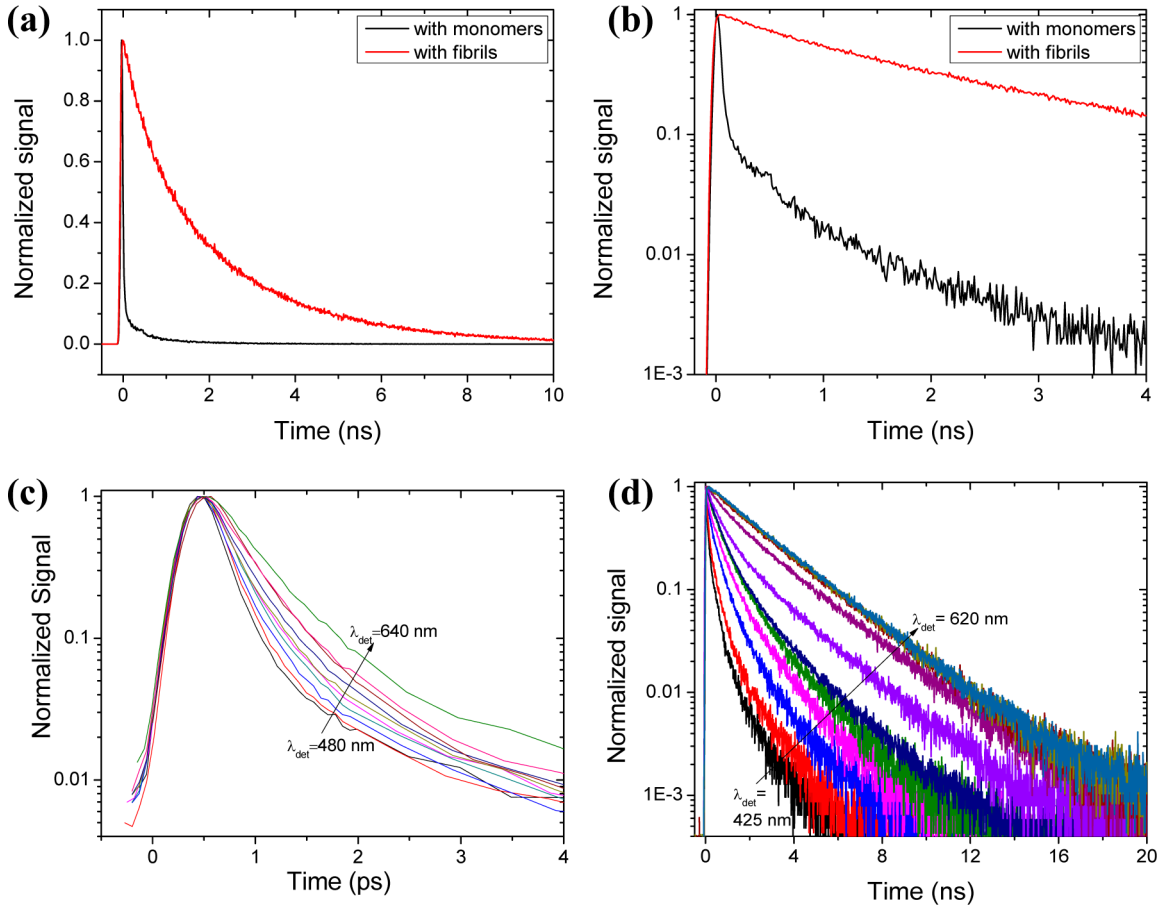

Figure 1. Time-resolved emission of AuO in the presence and absence of amyloid fibrils. TCSPC signal of AuO (~30 μM) with insulin (2 mg/mL) monomers (black curve) and fibrils (red curve) on (a) linear and (b) semilogarithmic scales. The dependence of the time-resolved emission on the detection wavelength of (c) AuO in water, measured by up-conversion, and (d) AuO in the presence of insulin fibrils, measured by TCSPC.

EXPERIMENTAL SECTION

Sample Preparation. A lyophilized powder of insulin (Recombinant Human insulin, ProSpec) was dissolved in a solution of 100 mM NaCl, pH 1.6, at a final insulin concentrations of 0.5–2 mg/mL. For fibril formation, the solution was heated to 65 °C for ~4 h without mechanical agitation. To avoid any seeding, preaggregation, and assembly, fresh and filtered solutions were prepared for each experiment. Stock solutions of ThT and AuO were prepared by dissolving them in water at a final concentration of 1 mM. The amyloidogenesis process was followed by two experimental methods: (1) 30 μL from the stock solution (of either ThT or AuO) was added to a 1.5 mL of the 2 mg/mL insulin solution (final concentration of AuO/ThT is 20 μM) immediately after dissolving the lyophilized powder and before heating, (2) 100 μL from the 0.5 mg/mL insulin solution was added to a preprepared AuO/ThT solution (pH 7, final AuO/ThT concentration of 35 μM)

Time-Resolved Emission. For excitation, we used a cavity-dumped Ti-sapphire femtosecond laser (Mira, Coherent), which provides short (120 fs) pulses of variable repetition rates, operating at the second-harmonic-generation (SHG) frequency (for both ThT and AuO excitation), spectral range of 380–420 nm, with a relatively low repetition rate of 800 kHz. The time-resolved emission of the bound (to insulin fibrils) AuO and ThT were obtained by the time-correlated single-photon-counting (TCSPC) technique. The TCSPC detection system is based on a Hamamatsu 3809U photomultiplier (PM), which collects the fluorescence that is spectrally selected by double monochromator operating in the nondispersive mode with a spectral width of 10 nm. The PM output was processed by Edinburgh Instruments TCC 900 computer module for TCSPC. The overall instrumental-response function was about 35 ps full-width at half-maximum (fwhm). The excitation-pulse energy was reduced by neutral-density filters to about 10 pJ. The time-resolved emission of unbound AuO was obtained by an up-conversion technique. The up-conversion system (FOG-100, CDP, Russia) was operated at 800 kHz. The samples were excited by pulses of ~8 mW on average at the SHG frequency. The time-response of the up-conversion system is evaluated by measuring the relatively strong Raman-Stokes line of water shifted by 3600 cm^{-1}. It was found that the fwhm of the signal is 280 fs. The sample was placed in a rotating optical cell to avoid degradation.

Steady-State Emission. The steady-state emission measurements were performed using FluoroMax-3 spectrofluorometer (Horiba Jobin Yvon, NJ, USA). A rectangular quartz cuvette with an optical path length of 10 × 4 mm was used.

UV–vis Absorption Measurements. The UV–vis absorption measurements were taken with a Cary 5000 UV–vis-NIR Spectrophotometer, using a 1 cm quartz cuvette.

Epifluorescence Microscopy. A Leica epifluorescence microscope was used for obtaining the fluorescence images of the dyed insulin fibrils. A glass slide was used as the surface in which the insulin fibrils were deposited on. Prior to the

dx.doi.org/10.1021/jp310232b | J. Phys. Chem. B 2012, 116, 13389–13395

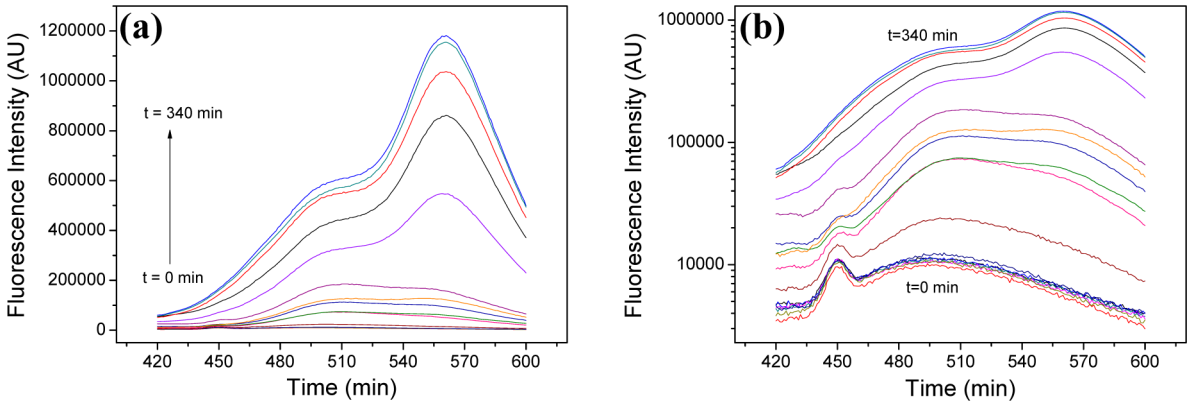

Figure 2. Steady-state emission of AuO. The change in the steady-state emission of AuO during the amyloidogenesis process, from t = 0 min and up to 240 min, on (a) linear and (b) semilogarithmic scales. The final solution concentrations were 0.2 mg/mL (32 μM) for insulin and 35 μM for AuO.

deposition the glass slide was cleaned by bath sonication by placing it in a vial containing iso-prpanol/acetone/ethanol (2 min in each). The insulin fibril solution with AuO or ThT (see the sample preparation section) was 10 times diluted in ddH_2O and drop-casted on top on the glass slide. A DAPI excitation filter was used for the excitation of the dyed fibrils (BP 340–380, Dichromatic mirror RKP 400, Suppression filter LP 425). The color image is a super position of three images, using blue, green and red filters.

RESULTS AND DISCUSSION

We used the amyloid fibril-forming protein of insulin as a protein model for following the kinetics of the amyloidogenesis process. Parts a and b of Figure 1 show the time-correlated single-photon-counting (TCSPC) time-resolved emission of a solution of AuO and insulin before and after the formation of the amyloid fibrils. As in the case of ThT, the emission lifetime of AuO also increases significantly upon binding to amyloid fibrils, from ~0.4 ps in the solution of insulin monomers (measured by an up-conversion technique), to 3 ns after the formation of insulin amyloid fibrils (measured by the TCSPC technique), an increase of more than 3 orders of magnitude in the lifetime of AuO. The time-resolved emission lifetime of AuO is highly sensitive to the detection wavelength (parts c and d of Figure 1 in the presence and absence of fibrils, respectively). Unlike similar wavelength-dependent lifetimes of many dyes, which are explained by solvation dynamics of the excited-state (prepared by a short laser pulse), the wavelength-dependent lifetimes of AuO should be interpreted differently. As in the case of ThT, the intramolecular rotation of the molecule causes a shift from the locally excited (higher energy) state to a CT (lower energy) state, which subsequently leads to a short emission lifetime, especially at short detection wavelengths.

Table 1. Average Lifetimes of AuO with Insulin As a Function of Time and Wavelength

time (min)	τ_{ave} @ 490 nm (ns)	τ_{ave} @ 560 nm (ns)
≤120	<0.06	<0.06
140	0.08	0.26
160	0.22	0.86
180	0.24	1.51
200	0.33	1.60
220	0.38	1.68
240	0.41	1.77
260	0.53	2.49
≥280	0.55	2.59

The primary requirement of a fluorescent marker for amyloid fibrils is to quantitatively follow the amyloidogenesis process, especially in order to quantify the potency of amyloid-fibril inhibitors. We used two experimental approaches in order to validate the use of AuO as a fluorescent marker for the formation of amyloid fibrils. The first approach, and the more common one for ThT, was to add an aliquot from the reaction tube (containing 0.5 mg/mL of insulin) to a cuvette or a microplate containing the solution of AuO (0.1 mM), so that the insulin is saturated by AuO (the results are shown in Figures 2 and 6). The second approach was to add AuO to the reaction tube (2 mg/mL of insulin, final AuO concentration of 30 μM, so as AuO is saturated by insulin) prior to the amyloidogenesis process (Figures S2 and S6 of the Supporting Information) and to follow the fluorescence of AuO as the process progresses.[26] These two experimental approaches yielded similar results.

The amyloidogenesis process of insulin fibrils, as those of other amyloid fibrils, begins with a lag phase that is followed by exponential growth up to the stationary stage.[27,28] Indeed, the steady-state emission of AuO (excited at 390 nm) during the amyloidogenesis process (part a of Figure 2) increases during the process up to the stationary phase. An important feature of the shape of the steady-state emission-spectrum curve of AuO can be seen by the shift in the position of the main emission peak as AuO binds to amyloid fibrils (part b of Figure 2). In the presence of insulin monomers, the low-intensity peak is located at 495 nm, however as AuO binds to amyloid fibrils a high-intensity peak forms at 560 nm. Table 1 shows the averaged lifetime (as measured by TCSPC) at the wavelengths of 490 and 560 nm during the amyloidogenesis process. The increase in AuO intensity together with a spectral shift in the position of the main emission peak has been observed in complexes of AuO with other molecules as well, such as DNA,[29] serum albumins,[30] alcohol dehydrogenase (ADH),[29,30] and $\alpha/\beta/\gamma$-cyclodextrins.[31] The increase in the fluorescence intensity ranges from slight, in the case of DNA,[29] to almost 2 orders of magnitude following complexation with ADH.[30] The position of the main emission peak of AuO ranged from 486 nm in n-butanol to 520 nm with ADH, whereas in water the peak position is at 506 nm.[30] Here, we show that, upon binding of

dx.doi.org/10.1021/jp310232b | J. Phys. Chem. B 2012, 116, 13389–13395

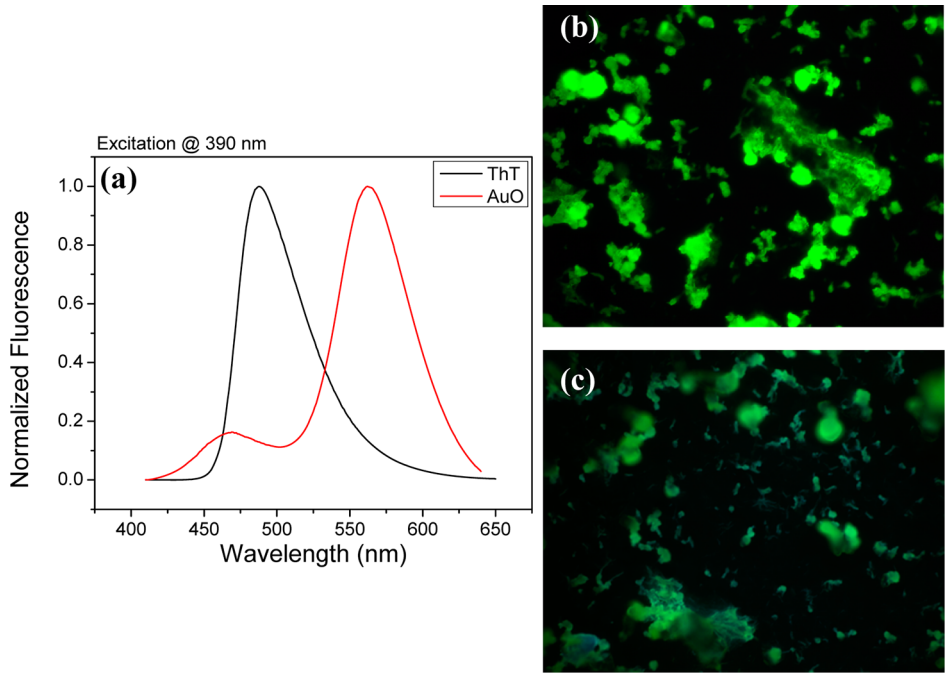

Figure 3. Comparison in the steady-state emission between AuO and ThT. (a) Steady-state spectrum of ThT (black curve) and AuO (red curve) in the presence of insulin fibrils. Fluorescence-microscopy images of insulin fibrils in the presence of (b) AuO and (c) ThT.

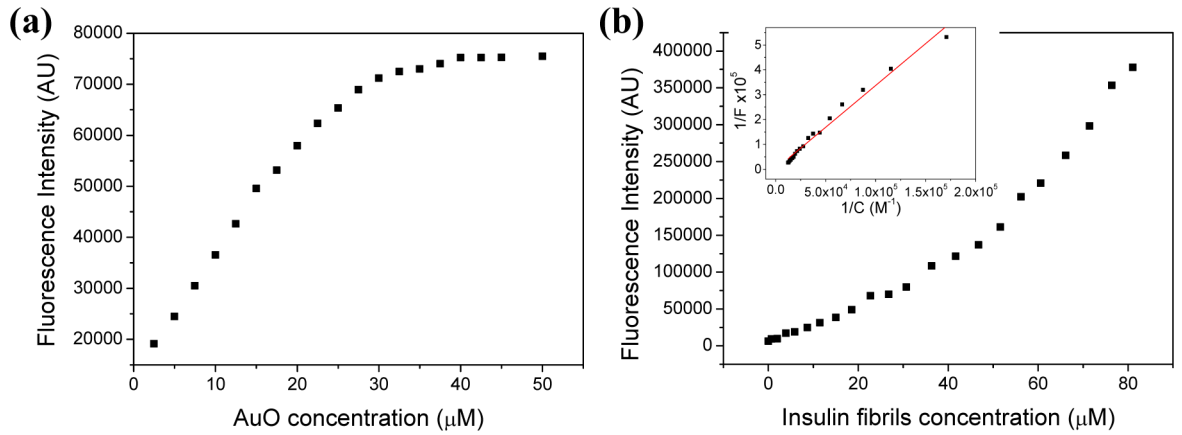

Figure 4. Titration curves of (a) AuO in a solution of insulin fibrils (150 μM), and (b) insulin fibrils in a solution of AuO (10 μM). The insert show a fit of $1/F$ vs $1/C$.

AuO to amyloid fibrils, the position of the main emission peak is significantly red-shifted to 560 nm and increases by 3 orders of magnitude. The spectral shift of AuO as it binds to proteins was explained by a polarizable binding environment.[30] The increase in the intensity, as in the case of ThT, is due to the inhibition of the intramolecular CT process, which was caused by the inhibition of the internal rotation within AuO (marked as arrows in Scheme 1) as it binds to amyloid fibrils. The difference in the steady-state emission-peak positions of ThT and AuO (part a of Figure 3) causes the dyed fibrils to exhibit different colors under the excitation of a fluorescence microscope. The AuO-dyed fibrils are more green (part b of Figure 3) and the ThT-dyed fibrils are more cyan (part c of Figure 3). We further estimate the anisotropy of the emission and the quantum yield (QY) of AuO in comparison to ThT. The QY estimation was calculated by comparing it to the recently reported QY of ThT at its bound state to insulin fibrils (0.83),[32] and by comparing the measured radiative lifetime of its bound state to the theoretical one that was calculated using the Strickler–Berg formula.[29,33] Whereas the anisotropy of AuO (measured at 560 nm) in its bound state is comparable to ThT, 0.22 for AuO (the anisotropy steady-state measurements are shown in Figure S3 of the Supporting Information) in comparison to the reported value of 0.27 for ThT,[34] the QY of AuO in its bound state is lower than ThT, and it is in the range of 0.2 (by comparing to ThT) to 0.26 (by using the Strickler–Berg formula).

To estimate the binding constant and stoichiometry of the binding process of AuO to insulin fibrils, we measured the change in the fluorescence intensity by both titrating a solution of insulin fibrils (150 μM) with AuO (part a of Figure 4) and by titrating a solution of AuO (10 μM) with insulin fibrils (part b of Figure 4). As seen in part a of Figure 4, the fluorescence intensity starts to saturate at ~38 μM of AuO, four folds lower than the insulin concentration. We used the data shown in part b of Figure 4 to estimate the fluorescent binding constant of

dx.doi.org/10.1021/jp310232b | J. Phys. Chem. B 2012, 116, 13389–13395

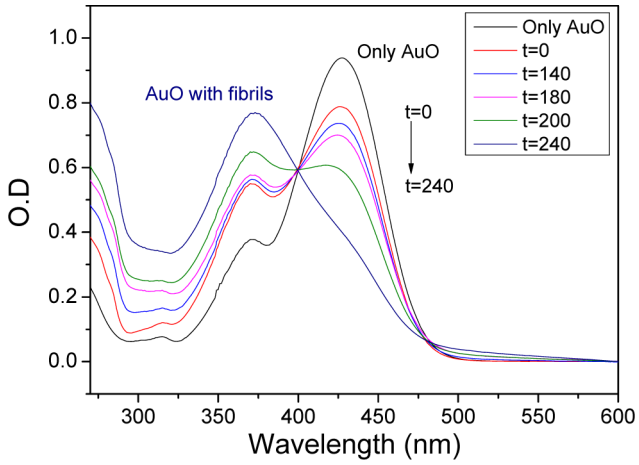

Figure 5. Absorption spectrum of free AuO (35 μM) in solution and in the presence of insulin (0.2 mg/mL) at several times point during the amyloidogenesis process.

insulin fibrils to AuO, by fitting it to $1/F = 1/F_{max} + (K_d/F_{max})(1/C)$, where F is the fluorescence intensity, F_{max} is the maximal fluorescence intensity, K_d is the dissociation constant and C in the concentration of the protein.[35] This method was previously used to determine the dissociation constant of AuO and ADH.[36,37] The straight line fit (The plot of $1/F$ vs $1/C$ is in the insert of part b of Figure 4) resulted in a dissociation constant of $K_d = 1.12 \times 10^{-6}$.

A possible explanation to the dual emission band of AuO-bound insulin fibril is that AuO is a photoacid, which means that the emission at 450 nm can be assigned to a protonated form, whereas the 560 nm band can be assigned to the deprotonated form. Photacids are weak acids in the ground-state with pK_a values ranging between 5 and 9. In their excited singlet state, however, their acidity increases by ~7 orders of magnitude. Upon excitation of the protonated form the acidity increases and proton transfer either to the solvent or to a mild base occurs within the excited-state lifetime. The excited-state-proton-transfer (ESPT) rate coefficient of protonated aniline in aqueous solution was found to be $1.4 \times 10^{10} s^{-1}$.[38] The nonradiative rate coefficient of AuO in water is larger than 10^{12} s^{-1} rendering the observation of ESPT in aqueous solution impossible. In contrast, on fibrils, where the nonradiative rate is slower by 3 orders of magnitude and the emission lifetime is 2.6 ns, the ESPT rate is faster than the effective radiative rate, so that the deprotonated form is seen in the steady-state spectrum at 560 nm.

Important to notice that the main emission peak at 560 nm is not sensitive to the pH at the range of pH 2−10 (part a of Figure S4 of the Supporting Information). However the second low-intensity peak, located at 500 nm, is pH-dependent and its intensity increases at pH ≥ 4. In this context, we observed that there is a difference in the steady-state emission spectrum shape between the two experimental procedures that were described before for following the amyloidogenesis process by AuO. Although the main emission peak is located at 560 nm, when we added aliquots from the insulin solution to the AuO solution the low intensity peak was located at 500 nm (Figure 2), and, when AuO was added to the insulin solution during the amyloidogenesis process, this low intensity peak was located at 470 nm and its intensity was very low (Figure S2 of the Supporting Information). The blue-shift of the high energy band, from 500 to 470 nm, can be explained by the hydrophobic environment of AuO when it is absorbed during the amyloidogenesis process.

To further describe the two states of AuO, we followed the amyloidogenesis process by measuring the UV−vis absorption as well (Figure 5). As shown in the figure, AuO exhibits an isosbestic point (at 400 nm) between its unbound mode (427 nm) and bound mode (373 nm). Unlike ThT, in which the absorption, excitation, and emission peak positions do not change much between its bound and unbound states (also, Figure S5 of the Supporting Information),[39,40] in AuO the absorption spectrum is blue-shifted, the excitation spectrum remains in the same location, and the emission spectrum is significantly red-shifted.

The common way to present the use of a fluorescent probe in order to follow the amyloidogenesis process is to track the probe emission at a certain wavelength (482 nm for ThT) as a function of time. Figure 6 shows the comparison between ThT and AuO as fluorescent probes for the formation of insulin fibrils, under the same experimental conditions (by adding aliquot of the insulin solution to a preprepared AuO or ThT solutions, the measurements in which the dye was present in the insulin solution during the process are shown in Figure S6 of the Supporting Information). As shown in the figure, both

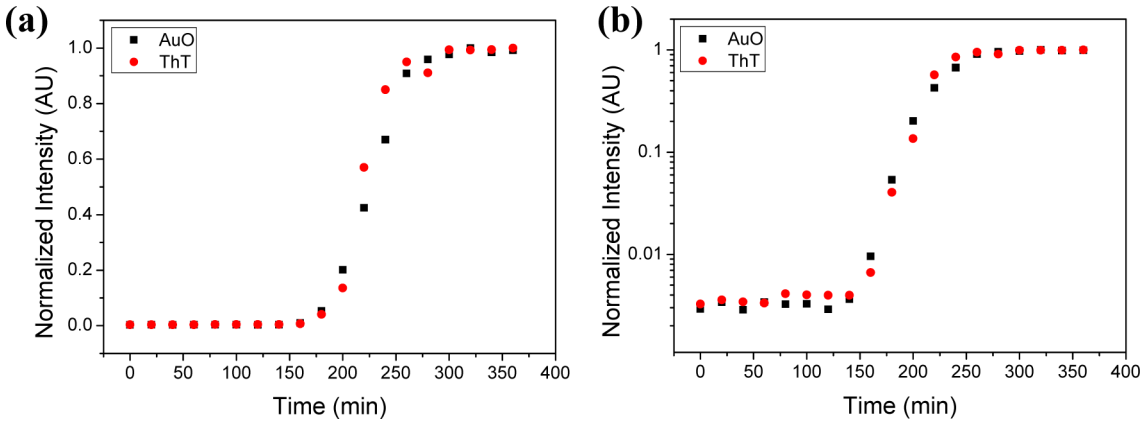

Figure 6. Kinetics of the amyloidogenesis process. The normalized main peak intensity as a function of time of AuO (λ_{ex} = 390 nm, λ_{em} = 562 nm) and ThT (λ_{ex} = 440 nm, λ_{em} = 487 nm) on (a) linear and (b) semilogarithmic scales. The final solution concentrations were 0.2 mg/mL (32 μM) for insulin and 35 μM for AuO or ThT.

dx.doi.org/10.1021/jp310232b | J. Phys. Chem. B 2012, 116, 13389−13395

on a linear (part a of Figure 6) and semilogarithmic (part b of Figure 6) scales, the results that were obtained by the use of AuO are highly similar to the results obtained with ThT, and thus validate its use as a fluorescent probe for the detection of amyloid fibrils. The results (with ThT) agree with the experimental results of insulin amyloidogenesis process[41] and to the kinetic models for amyloid fibrillization.[42] However, the large shift in the emission peak of AuO as it binds to amyloid fibrils, without a change in the excitation peak position (Figure S7 of the Supporting Information), introduces greater sensitivity to the measurements with AuO.

CONCLUSIONS

In conclusion, we introduce here the use of AuO as a fluorescent marker for the detection of amyloid fibrils. Although the use of AuO as a fluorescent probe for the amyloidogenesis process yields similar results as for ThT, it has desirable optical properties for a fluorescent marker. Those desirable properties manifest in a large peak separation, both in the emission and absorption spectra, between its bound and unbound states, in which the absorption peak position is blue-shifting by 54 nm, and the emission spectrum is red-shifting by 60 nm. The large change in the optical properties is explained by the photoacid activity of AuO. The dual band emission of AuO, in which the main emission band position (and thus the color of it) can be changed according to what molecule AuO binds to, can be further used in biological imaging of mainly amyloid fibrils, but probably to other, yet unexplored, biological molecules.

ASSOCIATED CONTENT

Supporting Information

Seven supplemental figures (citation report, additional spectroscopic analysis, and anisotropy). This material is available free of charge via the Internet at http://pubs.acs.org.

AUTHOR INFORMATION

Corresponding Author

*E-mail: amdursky@weizmann.ac.il (N.A.), dhuppert@post.tau.ac.il (D.H.).

Notes

Notes. The authors declare no competing financial interest. The authors declare no competing financial interest.

ACKNOWLEDGMENTS

This work was supported by grants from the James-Franck German-Israeli Program in Laser-Matter Interaction. N.A thanks the Clore scholars program for financial assistance.

REFERENCES

(1) Naiki, H.; Higuchi, K.; Hosokawa, M.; Takeda, T. Fluorometric-determination of amyloid fibrils invitro using the fluorescent dye, thioflavine-T. *Anal. Biochem.* **1989**, *177*, 244−249.

(2) Klunk, W. E.; Wang, Y. M.; Huang, G. F.; Debnath, M. L.; Holt, D. P.; Mathis, C. A. Uncharged thioflavin-T derivatives bind to amyloid-beta protein with high affinity and readily enter the brain. *Life Sci.* **2001**, *69*, 1471−1484.

(3) Mathis, C. A.; Bacskai, B. J.; Kajdasz, S. T.; McLellan, M. E.; Frosch, M. P.; Hyman, B. T.; Holt, D. P.; Wang, Y. M.; Huang, G. F.; Debnath, M. L.; Klunk, W. E. A lipophilic thioflavin-T derivative for positron emission tomography (PET) Imaging of amyloid in brain. *Bioorg. Med. Chem. Lett.* **2002**, *12*, 295−298.

(4) LeVine, H. Quantification of beta-sheet amyloid fibril structures with thioflavin T. *Methods Enzymol.* **1999**, *309*, 274−284.

(5) Ban, T.; Hamada, D.; Hasegawa, K.; Naiki, H.; Goto, Y. Direct observation of amyloid fibril growth monitored by thioflavin T fluorescence. *J. Biol. Chem.* **2003**, *278*, 16462−16465.

(6) Bulic, B.; Pickhardt, M.; Schmidt, B.; Mandelkow, E. M.; Waldmann, H.; Mandelkow, E. Development of tau aggregation inhibitors for Alzheimer's Disease. *Angew. Chem., Int. Ed.* **2009**, *48*, 1741−1752.

(7) Biancalana, M.; Koide, S. Molecular mechanism of thioflavin-T binding to amyloid fibrils. *Biochim. Biophys. Acta, Proteins Proteomics* **2010**, *1804*, 1405−1412.

(8) Celej, M. S.; Jares-Erijman, E. A.; Jovin, T. M. Fluorescent *N*-arylaminonaphthalene sulfonate probes for amyloid aggregation of alpha-synuclein. *Biophys. J.* **2008**, *94*, 4867−4879.

(9) W. Bertoncini, C.; Celej, M. S. Small molecule fluorescent probes for the detection of amyloid self-assembly in vitro and in vivo. *Current Protein and Peptide Science* **2011**, *12*, 206−220.

(10) Lindgren, M.; Hammarström, P. Amyloid oligomers: Spectroscopic characterization of amyloidogenic protein states. *FEBS Journal* **2010**, *277*, 1380−1388.

(11) Hong, Y.; Meng, L.; Chen, S.; Leung, C. W. T.; Da, L.-T.; Faisal, M.; Silva, D.-A.; Liu, J.; Lam, J. W. Y.; Huang, X.; Tang, B. Z. Monitoring and inhibition of insulin fibrillation by a small organic fluorogen with aggregation-induced emission characteristics. *J. Am. Chem. Soc.* **2011**, *134*, 1680−1689.

(12) Erez, Y.; Liu, Y. H.; Amdursky, N.; Huppert, D. Modeling the nonradiative-decay rate of electronically-excited ThT. *J. Phys. Chem. A* **2011**, *115*, 8479−8487.

(13) Singh, P. K.; Kumbhakar, M.; Pal, H.; Nath, S. Ultrafast bond twisting dynamics in amyloid fibril sensor. *J. Phys. Chem. B* **2010**, *114*, 2541−2546.

(14) Singh, P. K.; Kumbhakar, M.; Pal, H.; Nath, S. Viscosity effect on the ultrafast bond twisting dynamics in an amyloid fibril sensor: Thioflavin-T. *J. Phys. Chem. B* **2010**, *114*, 5920−5927.

(15) Stsiapura, V. I.; Maskevich, A. A.; Kuzmitsky, V. A.; Uversky, V. N.; Kuznetsova, I. M.; Turoverov, K. K. Thioflavin T as a molecular rotor: Fluorescent properties of thioflavin T in solvents with different viscosity. *J. Phys. Chem. B* **2008**, *112*, 15893−15902.

(16) Amdursky, N.; Gepshtein, R.; Erez, Y.; Huppert, D. Temperature dependence of the fluorescence properties of thioflavin-T in propanol, a glass-forming liquid. *J. Phys. Chem. A* **2011**, *115*, 2540−2548.

(17) Amdursky, N.; Gepshtein, R.; Erez, Y.; Koifman, N.; Huppert, D. Pressure effect on the nonradiative process of thioflavin-T. *J. Phys. Chem. A* **2011**, *115*, 6481−6487.

(18) Hutter, T.; Amdursky, N.; Gepshtein, R.; Elliott, S. R.; Huppert, D. Study of thioflavin-T immobilized in porous silicon and the effect of different organic vapours on the fluorescence lifetime. *Langmuir* **2011**, *27*, 7587−7594.

(19) Naik, L. R.; Naik, A. B.; Pal, H. Steady-state and time-resolved emission studies of thioflavin-T. *J. Photochem. Photobiol., A* **2009**, *204*, 161−167.

(20) Singh, P. K.; Kumbhakar, M.; Pal, H.; Nath, S. Ultrafast torsional dynamics of protein binding dye thioflavin-T in nano-confined water pool. *J. Phys. Chem. B* **2009**, *113*, 8532−8538.

(21) Stsiapura, V. I.; Maskevich, A. A.; Tikhomirov, S. A.; Buganov, O. V. Charge transfer process determines ultrafast excited state deactivation of thioflavin T in low-viscosity solvents. *J. Phys. Chem. A* **2010**, *114*, 8345−8350.

(22) Glasbeek, M.; Zhang, H. Femtosecond studies of solvation and intramolecular configurational dynamics of fluorophores in liquid solution. *Chem. Rev.* **2004**, *104*, 1929−1954.

(23) van der Meer, M. J.; Zhang, H.; Glasbeek, M. Femtosecond fluorescence upconversion studies of barrierless bond twisting of auramine in solution. *J. Chem. Phys.* **2000**, *112*, 2878−2887.

(24) Rogers, D. R. Screening for amyloid with thioflavin-T fluorescent method. *Am. J. Clin. Pathol.* **1965**, *44*, 59.

(25) Conrad, R. H.; Heitz, J. R.; Brand, L. Characterization of a fluorescent complex between auramine-o and horse liver alcohol dehydrogenase. *Biochemistry* **1970**, *9*, 1540-&.
(26) Tao, N. J. Probing potential-tuned resonant tunneling through redox molecules with scanning tunneling microscopy. *Phys. Rev. Lett.* **1996**, *76*, 4066−4069.
(27) Bhak, G.; Choe, Y. J.; Paik, S. R. Mechanism of amyloidogenesis: Nucleation-dependent fibrillation versus double-concerted fibrillation. *BMB Rep.* **2009**, *42*, 541−551.
(28) Chiti, F.; Dobson, C. M. Protein misfolding, functional amyloid, and human disease. *Annu. Rev. Biochem.* **2006**, *75*, 333−366.
(29) Gautam, P.; Harriman, A. Internal-rotation in auramine-o. *J. Chem. Soc., Faraday Trans.* **1994**, *90*, 697−701.
(30) Chen, R. F. Fluorescence of free and protein-bound auramine o. *Arch. Biochem. Biophys.* **1977**, *179*, 672−681.
(31) Mwalupindi, A. G.; Rideau, A.; Agbaria, R. A.; Warner, I. M. Influence of organized media on the absorption and fluorescence-spectra of auramine-o dye. *Talanta* **1994**, *41*, 599−609.
(32) Kuznetsova, I. M.; Sulatskaya, A. I.; Uversky, V. N.; Turoverov, K. K. Analyzing thioflavin T binding to amyloid fibrils by an equilibrium microdialysis-based technique. *PLoS One* **2012**, *7*, e30724.
(33) Strickler, S. J.; Berg, R. A. Relationship between absorption intensity and fluorescence lifetime of molecules. *J. Chem. Phys.* **1962**, *37*, 814−822.
(34) Sabate, R.; Saupe, S. J. Thioflavin T fluorescence anisotropy: An alternative technique for the study of amyloid aggregation. *Biochem. Biophys. Res. Commun.* **2007**, *360*, 135−138.
(35) Wang, J. L.; Edelman, G. M. Fluorescent probes for conformational states of proteins. *J. Biol. Chem.* **1971**, *246*, 1185−1191.
(36) Conrad, R. H.; Heitz, J. R.; Brand, L. Characterization of a fluorescent complex between auramine O and horse liver alcohol dehydrogenase. *Biochemistry* **1970**, *9*, 1540−1546.
(37) Sigman, D. S.; Glazer, A. N. The site of auramine O binding to horse liver alcohol dehydrogenase. *J. Biol. Chem.* **1972**, *247*, 334−341.
(38) Tajima, S.; Shiobara, S.; Shizuka, H.; Tobita, S. Excited-state proton-dissociation of *N*-alkylated anilinium ions in aqueous solution studied by picosecond fluorescence measurements. *Phys. Chem. Chem. Phys.* **2002**, *4*, 3376−3382.
(39) Hatters, D. M.; MacPhee, C. E.; Lawrence, L. J.; Sawyer, W. H.; Howlett, G. J. Human apolipoprotein C-II forms twisted amyloid ribbons and Closed Loops†. *Biochemistry* **2000**, *39*, 8276−8283.
(40) Maskevich, A. A.; Stsiapura, V. I.; Kuzmitsky, V. A.; Kuznetsova, I. M.; Povarova, O. I.; Uversky, V. N.; Turoverov, K. K. Spectral properties of thioflavin t in solvents with different dielectric properties and in a fibril-incorporated form. *J. Proteome Res.* **2007**, *6*, 1392−1401.
(41) Manno, M.; Craparo, E. F.; Martorana, V.; Bulone, D.; San Biagio, P. L. Kinetics of insulin aggregation: Disentanglement of amyloid fibrillation from large-size cluster formation. *Biophys. J.* **2006**, *90*, 4585−4591.
(42) Morris, A. M.; Watzky, M. A.; Finke, R. G. Protein aggregation kinetics, mechanism, and curve-fitting: A review of the literature. *Biochim. Biophys. Acta, Proteins Proteomics* **2009**, *1794*, 375−397.